X-Ray and NMR Studies on Host–Guest Inclusion Complex Formation between Crown Ethers and Pyridinium Compounds

Markku Lämsä,* Juhani Huuskonen, Kari Rissanen, and Jouni Pursiainen

Abstract: Inclusion complex formation between benzene-substituted crown ethers and electron-deficient pyridinium ions was studied by crystallographic and NMR methods. The major attractive host–guest interactions in these complexes are face-to-face aromatic–aromatic and cation–π interactions. In addition, the crystal structures show that hydrogen bonding influences the complexation of cations. Individual studies of the binding strength as a function of host, guest, and solvent were carried out. Four pyridinium guests were prepared for the investigation. Fast atom bombardment (FAB) mass spectrometry was used to determine the stoichiometry of the complexes. The stability constants were measured by ^{1}H NMR and the structures of the complexes in acetonitrile are discussed. X-ray crystal structures were determined for complexes of dibenzo-18-crown-6 with pyridinium tetrafluoroborate (2B18C6–$PyBF_4$) and dibenzo-18-crown-6 with 1-aminopyridinium tetrafluoroborate (2B18C6–1-NH_2PyBF_4).

Keywords: crown compounds · cations · host–guest chemistry · pi interactions

Introduction

The complexation of cationic substrates with macrocyclic receptors has been the subject of much interest in recent years. Molecular complexes are usually held together by hydrogen bonding, ion pairing, π-acid to π-base interactions, metal–ligand binding, van der Waals forces, solvent reorganization, or partial covalent bonds. In inclusion complexes in which an organic substrate is incorporated into a host cavity, the predominant attractive host–guest interactions are the dipole–dipole, dipole–induced dipole, or induced dipole–induced dipole van der Waals forces. Face-to-face and edge-to-face interactions between aromatic rings of the two binding species are another stabilizing interaction, which is usually discussed separately from the van der Waals term.[1]

Recently, specific interactions of guests with π-donor systems have attracted interest with regard to biological processes. Interactions between aromatic rings play an important role, for example, in controlling the conformations and substrate-binding properties of nucleic acids and proteins.[2] Extensive theoretical[2,3] and experimental studies[4] have been made of the π–π interactions that stabilize synthetic host–guest complexes. Additionally, the exploitation of complexes between crown ethers and bipyridinium dications (paraquat, diquat)[5] in self-assembly processes has attracted attention.[6] In the above complexes, an additional binding force, the cation–π effect, contributes to the stability. The cation–π effect was observed by Lehn et al.[7] and by Dougherty et al.,[8] and it has been of increasing interest in enzyme–ligand interactions. An example is the interaction between acetylcholine and its esterase.[8,9] This type of donor–acceptor interaction also exists between electron-rich aromatic receptors and electron-deficient (cationic) guests.[4d,10]

We have previously observed that π–π stacking and cation–π interactions play a significant role in the complexation between benzene-substituted crown ethers and electron-deficient aromatic carbenium ions such as the tropylium ion.[11] Here we report on our studies of the analogous complexation of pyridinium ions, which provide further information on the nature of the complexation between carbenium cations and macrocycles.

Pyridinium salts are both aromatic carbenium ions and iminium ions. An essential biochemical process associated with the pyridinium ion is the enzyme-mediated exchange of hydride between NADH and $NADP^+$.[12] The chemical transformation involves a transfer of hydride from 1,4-dihydropyridine to a pyridinium salt. Likewise, reduction by hydride and reversible hydride transfer between tropylium ions and

[*] Dr. Lämsä, Assoc. Prof. Dr. J. Pursiainen
Department of Chemistry, University of Oulu
Linnanmaa, P.O. Box 333, FIN-90571 Oulu (Finland)
Fax: Int. code + 358 8 5531603
e-mail: mlamsa@cc.oulu.fi

Dr. J. Huuskonen, Prof. Dr. K. Rissanen
Department of Chemistry, University of Jyväskylä
P.O. Box 35, FIN-40351 Jyväskylä (Finland)
Fax: Int. code + 358 14 602501

0947-6539/98/0401-0084 $ 17.50+.50/0

substituted cycloheptatriene is an interesting reaction of the tropylium ion.[13]

The host–guest complexation of a macrocyclic ligand with a pyridinium ion has been studied on several occasions previously. Piepers and Kellogg observed in 1980 that pyridine-substituted crown ethers form complexes with *n*-alkylpyridinium salts.[14] Some pyridinium salts, together with other quaternary ammonium compounds, have been used as guests in complexation studies with cyclophane[4d,8b,15] and calixarene[10a,16] hosts. The 1:1 complex between 18-crown-6 and pyridinium chlorochromate has been prepared in order to study its oxidation properties towards alcohols.[17] New catenanes and rotaxanes have been assembled on the basis of donor–acceptor interactions between bipyridinium ions and benzo and naphthalene crown ethers.[6] In spite of extensive studies of *n*-alkylpyridinium salts by LD, FD, and FAB mass spectrometry, according to Laali there are no gas-phase host–guest studies on crown–pyridinium systems.[18]

Here we describe binding studies on benzene-substituted crown ethers and pyridinium salts in the gas phase and in solution, with characterization of the complexes by FABMS and ^{1}H NMR spectroscopy. Furthermore, we report crystal structures for inclusion complexes of pyridinium tetrafluoroborate and 1-aminopyridinium tetrafluoroborate with dibenzo-18-crown-6 (2B18C6).

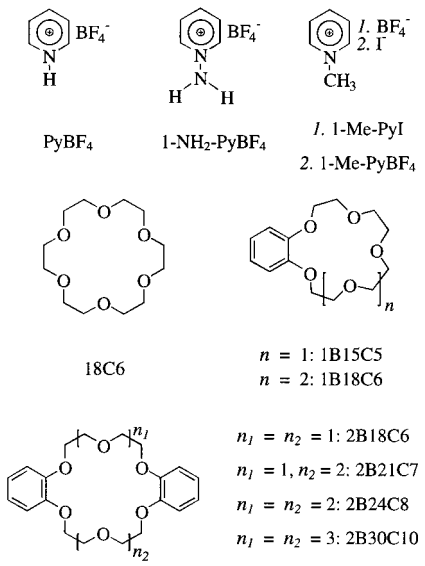

Results and Discussion

FAB mass spectrometry and complexation in the gas phase: Since 1981, fast atom bombardment mass spectrometry (FABMS) has been widely utilized for the detection of 1:1 adducts. During the last five years, it has also been systematically applied in the field of host–guest complexation chemistry and to more weakly bonded complexes.[19] Receptor–ligand (enzyme–substrate) associations have been identified, for example.[20] We have used FABMS as a preliminary test for the formation of complexes between host and guest.[21]

The mass spectrum of pyridinium tetrafluoroborate in the presence of dibenzo-18-crown-6 (2B-18-C6) is presented as an example in Figure 1. The FABMS results provide clear evidence for complex formation between crown ethers and pyridinium ions in the gas phase. Peaks at $m/z = 80$, 360, and 440 correspond to the pyridinium cation without counteranion, uncomplexed crown ether, and the 1:1 complex after loss of its BF_4^- ion, respectively. The FABMS results are summarized in Table 1. All spectra exhibit peaks at $m/z = 154$, 136, and 107, which originate from the NBA matrix, and cleavage ions at $m/z = 45$, 89, 133, and 177 due to formation of $(C_2H_4O)_n$ fragments from the crown ether. In addition, the presence of a small amount of sodium impurity (from glassware) led to crown ether–Na^+ adduct peaks in several experiments. The absence of peaks for complexes higher than 1:1 in any FABMS spectrum indicates preferential formation of 1:1 complexes in the gas phase.

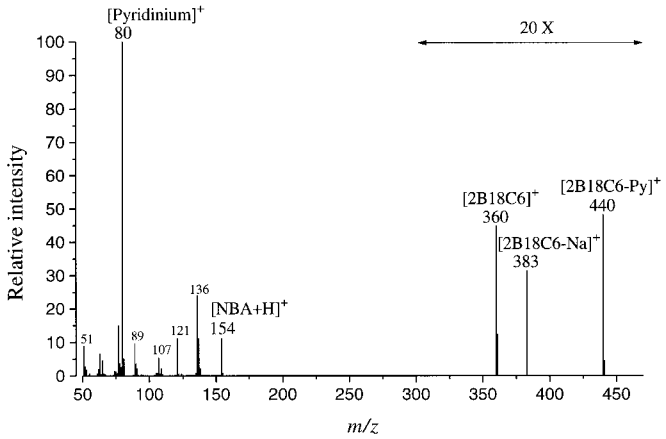

Figure 1. Positive-ion FAB mass spectrum for a mixture of 2B18C6 and pyridinium tetrafluoroborate (1:1) in an NBA matrix.

The mostly low intensity of the complex peaks, less than about 4% of the height of the base peak (frequently a pyridinium guest ion), suggests that complexation is weak. The interaction energies involved in aromatic association tend to be low, and this suggests that complexation between

Abstract in Finnish: *Työssä tutkittiin bentseenisubstituoitujen kruunueettereiden kompleksoitumista pyridiniumionien kanssa röntgendiffraktion ja NMR:n avulla. Kruunueetterit muodostivat pyridiniumionien kanssa inkluusiokomplekseja. Näissä isäntä-vierasvuorovaikutus perustui pääosin vastakkaisten aromaattisten yksikköjen väliseen ja kationi-π-vuorovaikutukseen. Lisäksi kiderakenteet paljastivat, että vetysidoksilla oli vaikutusta kationien sitoutumisessa. Kompleksoitumista tutkittiin isännän, vieraan ja liuottimen funktiona. Näitä tutkimuksia varten valmistettiin neljä pyridiniumyhdistettä. FAB-massaspektrometriaa käytettiin kompleksien stoikiometrian määrittämiseen. Stabiilisuusvakiot mitattiin ^{1}H NMR:n avulla ja tulosten perusteella arvioitiin kompleksien rakenteet asetonitriilissä. Dibentso-18-kruunu-6-pyridiniumtetrafluoroboraatin ja dibentso-18-kruunu-6-1-amiinipyridiniumtetrafluoroboraatin kiderakenteet määritettiin röntgendiffraktion avulla.*

Table 1. Partial positive ion FAB mass spectra of pyridinium salts in the presence of crown ethers (1:1 mixture) in NBA matrix.

	m/z (relative abundance /%) ion
pyridinium tetrafluoroborate	
1B15C5	77 (5.3) $C_6H_5^+$, 80 (100) Py^+, 154 (1.3) $[NBA+H]^+$, 247 (0.7) $(Py^+)_2BF_4^-$, 268 (7.6) $[1B15C5]^+$, 291 (1.7) $[1B15C5-Na]^+$, 348 (2.9) $[1B15C5-Py]^+$
1B18C6	77 (4.3) $C_6H_5^+$, 80 (100) Py^+, 247 (0.9) $(Py^+)_2BF_4^-$, 312 (2.8) $[1B18C6]^+$, 335 (0.5) $[1B18C6-Na]^+$, 393 (1.5) $[(1B18C6-Py)+H]^+$
2B18C6	77 (15.3) $C_6H_5^+$, 80 (100) Py^+, 154 (11.2) $[NBA+H]^+$, 360 (2.2) $[2B18C6]^+$, 383 (1.6) $[2B18C6-Na]^+$, 440 (2.4) $[2B18C6-Py]^+$
2B21C7	77 (9.9) $C_6H_5^+$, 80 (100) Py^+, 154 (1.6) $[NBA+H]^+$, 247 (0.9) $(Py^+)_2BF_4^-$, 404 (2.2) $[2B21C7]^+$, 484 (2.0) $[2B21C7Py]^+$
2B24C8	77 (5.3) $C_6H_5^+$, 80 (100) Py^+, 448 (0.3) $[2B24C8]^+$, 471 (0.2) $[2B24C8-Na]^+$, 529 (0.3) $[(2B24C8-Py)+H]^+$
2B30C10	77 (5.8) $C_6H_5^+$, 80 (100) Py^+, 154 (0.2) $[NBA+H]^+$, 247 (0.7) $(Py^+)_2BF_4^-$, 537 (0.3) $[2B30C10+H]^+$, 559 (0.3) $[2B30C10-Na]^+$, 617 (0.3) $[(2B30C10-Py)+H]^+$
18C6	80 (100) Py^+, 247 (2.5) $(Py^+)_2BF_4^-$, 265 (0.4) $[18C6+H]^+$, 287 (1.6) $[18C6-Na]^+$, 344 (3.7) $[18C6-Py]^+$
1-aminopyridinium tetrafluoroborate	
1B18C6	77 (8.4) $C_6H_5^+$, 95 (100) NH_2Py^+, 277 (4.0) $(NH_2Py^+)_2BF_4^-$, 312 (0.9) $[1B18C6]^+$, 407 (0.3) $[1B18C6-NH_2Py]^+$
2B18C6	77 (20.2) $C_6H_5^+$, 95 (100) NH_2Py^+, 154 (18,8) $[NBA+H]^+$, 360 (0.9) $[2B18C6]^+$, 383 (2.9) $[2B18C6-Na]^+$, 455 (1.1) $[2B18C6-NH_2Py]^+$
2B21C7	77 (9.7) $C_6H_5^+$, 95 (100) NH_2Py^+, 154 (0.9) $[NBA+H]^+$, 277 (2.5) $(NH_2Py^+)_2BF_4^-$, 404 (0.3) $[2B21C7]^+$, 499 (0.2) $[2B21C7-NH_2Py]^+$
2B24C8	77 (16.4) $C_6H_5^+$, 95 (100) NH_2Py^+, 154 (2.2) $[NBA+H]^+$, 277 (0.4) $(NH_2Py^+)_2BF_4^-$, 448 (1.2) $[2B24C8]^+$, 471 (<0.1) $[2B24C8-Na]^+$, 544 (0.6) $[(2B24C8-NH_2Py)+H]^+$
2B30C10	77 (8.4) $C_6H_5^+$, 95 (100) NH_2Py^+, 154 (4.1) $[NBA+H]^+$, 277 (1.5) $(NH_2Py^+)_2BF_4^-$, 537 (0.9) $[2B24C8+H]^+$, 559 $(Na]^+$, 630 (1.3) $[(2B24C8-NH_2Py)-H]^+$
18C6	95 (100) NH_2Py^+, 154 (1.3) $[NBA+H]^+$, 265 (0.7) $[18C6+H]^+$, 277 (1.9) $(Py^+)_2BF_4^-$, 359 (0.1) $[18C6-NH_2Py]^+$
1-methylpyridinium tetrafluoroborate	
1B18C6	77 (5.7) $C_6H_5^+$, 94 (100) $MePy^+$, 154 (1.4) $[NBA+H]^+$, 275 (1.7) $(MePy^+)_2BF_4^-$, 312 (2.5) $[1B18C6]^+$, 406 (0.1) $[1B18C6-MePy]^+$
2B18C6	77 (17.9) $C_6H_5^+$, 94 (100) $MePy^+$, 154 (15.1) $[NBA+H]^+$, 275 (0.6) $(MePy^+)_2BF_4^-$, 360 (2.9) $[2B18C6]^+$, 454 (0.6) $[2B18C6-MePy]^+$
2B21C7	77 (10.6) $C_6H_5^+$, 94 (100) $MePy^+$, 154 (2.8) $[NBA+H]^+$, 275 (3.1) $(MePy^+)_2BF_4^-$, 404 (1.1) $[2B21C7]^+$, 498 (0.1) $[2B21C7-MePy]^+$
2B24C8	77 (6.5) $C_6H_5^+$, 94 (100) $MePy^+$, 154 (1.3) $[NBA+H]^+$, 275 (1.1) $(MePy^+)_2BF_4^-$, 448 (0.2) $[2B24C8]^+$, 471 (0.4) $[2B24C8-Na]^+$, 542 (0.2) $[(2B24C8-MePy)]^+$

benzene-substituted crown ethers and pyridinium ions in the gas phase is stabilized by weak $\pi-\pi$ and cation $-\pi$ interactions. In addition, the formation of complexes between 18C6 and pyridinium ions shows that hydrogen bonding contributes to the stability of complexes. Comparison of the observed intensities of complex peaks suggests that pyridinium ion forms more stable complexes with crown ethers than do substituted pyridinium salts ($Py^+ > PyNH_2^+ > PyCH_3^+$) and that complexes of monobenzo-substituted crown ethers are somewhat more stable than those of disubstituted crown ethers.

The FABMS results are in good accord with our earlier work[20] and with the NMR and X-ray results reported below. However, interpretation of the results to yield quantitative thermochemical information is not straightforward since the relative peak intensities from FABMS probably do not fully reflect equilibrium conditions.[22]

^{1}H NMR titration and complexation in solution: The nature of the complexation in solution was studied by ^{1}H NMR spectroscopy. At room temperature rapid exchange between complexed and uncomplexed species is observed on the NMR time-scale at 200 MHz. The ^{1}H NMR experiments involved titration of a guest solution into a host solution until no significant change in the chemical shift was observed in successive NMR spectra. In the cases studied, increasing the host/guest molar ratio gradually shifted the signals of the pyridinium protons, but the chemical shift did not reach a limiting value even at high molar ratios. This indicates the formation of a weak complex with a low K_a value and also limited accuracy of the NMR titration technique.[23]

^{1}H NMR spectra provided several signals for independent K_a evaluations. The ^{1}H NMR spectra of pyridinium tetrafluoroborates consist of three separate peak patterns at about $\delta = 8-8.7$ for ring protons and separate signals for the NH_2 or CH_3 substituent. When benzene-substituted crown ether was added to a solution of pyridinium ion in CD_3CN, an upfield shift was observed for the resonances of the H4 and H3,5 protons. We postulate that the upfield shift is due to the aromatic ring currents of the benzene rings. The stability constants for complexation are calculated directly from the chemical shift differences of the pyridinium ring protons in the crown complexes and in the free form by Equation (1). The chemical shift differences of pyridinium ions are a linear function of 1/[crown ether]; this indicates 1:1 stoichiometry and rapid cation exchange.[24] Table 2 lists the stability constants and limiting upfield shifts of complexes calculated

Table 2. Stability constants and limiting upfield shifts[a] for the interaction of crown ethers with pyridinium ions in CD_3CN solution at 298 K measured by ^{1}H NMR titration.

	K_a /dm^{3}mol^{-1}	$\Delta\delta_C$	Norm[b]
pyridinium tetrafluoroborate			
1B15C5	46 ± 9	0.26 ± 0.02	0.0164
1B18C6	96 ± 6	0.32 ± 0.01	0.0100
2B18C6	33 ± 4	0.56 ± 0.03	0.0377
2B21C7	22 ± 4	0.63 ± 0.06	0.0206
2B24C8	19.2 ± 0.3	0.71 ± 0.01	0.0020
2B30C10	28 ± 5	0.46 ± 0.04	0.0170
18C6	113 ± 10	-0.24 ± 0.01	0.0060
1-aminopyridinium tetrafluoroborate			
1B18C6	33 ± 1	0.54 ± 0.01	0.0081
2B18C6	13 ± 2	1.14 ± 0.13	0.0346
2B21C7	5.7 ± 0.3	0.85 ± 0.04	0.0020
1-methylpyridinium tetrafluoroborate			
2B18C6	9 ± 1	0.15 ± 0.02	0.0010
2B21C7	10 ± 5	0.25 ± 0.14[c]	$r^2 = 0.96$[d]

[a] The $\Delta\delta_C$ values indicated relate to the chemical shift changes experienced by probe protons (H-4 for pyridinium ions) on 1:1 complexation. [b] The norm represents the closeness of fit of iteration; numerically, it is the square root of the sum of squares of the residuals. [c] The use of Equation (2) may lead to incorrect values of $\Delta\delta_C$ in systems where the stability constants are small because of an extrapolation. [d] Regression correlation (r^2) for Benesi – Hildebrand plot.

0947-6539/98/0401-0086 $ 17.50+.50/0 *Chem. Eur. J.* **1998**, *4*, No. 1

from the pyridinium H4 chemical shift by a nonlinear least-squares curve-fitting procedure. The stability constants calculated from the pyridinium H4 and H3,5 chemical shifts are the same (within 3–15%). The complexation-induced shift for the pyridinium H2,6 protons (except with 18C6) was very small ($\Delta\delta < 0.1$), and the calculated stability constants did not agree with the K_a values calculated from the H4 chemical shift. Evaluation of stability constants from chemical shifts of the crown ethers was not possible since no shift occurred in the presence of a guest molecule. This result was expected since the concentration of host was always at least ten times greater than the concentration of guest.

The ^{1}H NMR data indicate the formation of inclusion complexes between benzo-substituted crown ethers and pyridinium ions in CD_3CN. In these 1:1 complexes the most significant chemical shift changes are experienced by the H4 and H3,5 protons on the pyridinium ring. The sign of the chemical shift difference of the H2,6 protons on complexation depended on the size of the macrocycle: a small downfield shift was observed when the macrocycle ring contained less than 21 atoms, and an upfield shift when it contained more than 21 atoms. In addition, the ^{1}H NMR spectra of the complexes between crown ethers and 1-aminopyridinium tetrafluoroborate revealed a notable downfield shift for the NH_2 protons on complexation in CD_3CN. The stability constants calculated from the pyridinium H4 and NH_2 chemical shifts were comparable. Evidently the complex is also stabilized by N–H···O hydrogen bonding. The ^{1}H NMR results established that the electron-deficient pyridinium ion is wrapped by benzene-substituted crown ethers in a similar manner in solution as in the solid state. The data suggest that pyridinium ions are oriented face-to-face, such that the phenyl ring(s) and N–H, N–NH_2, and N–CH_3 substituents point away from the cavity of the crown ethers. The orientation may have its origin in the distribution of electron density in the pyridinium ring.

In an attempt to shed light on the charge separation and the dipole moment of pyridinium ions, we carried out ab initio calculations for the pyridinium cations. The calculations involve Hartree–Fock (HF) treatments with RHF/3-21G* basis sets at optimized geometries with Spartan 4.0.2b.[25] The dipole moment from formal charges of 1.99 D for pyridinium supports structures with some charge separation. The presence of an amino group at the N atom will decrease this charge separation, and thus the 1-aminopyridinium ion has a dipole moment of only 1.53 D. The effect of the methyl group can be expected to be similar since an alkyl group is electron-donating relative to a hydrogen atom. The calculated dipole moment of 1-methylpyridinium is 1.38 D. Thus the substituents decrease the positive charge on the pyridinium ring and reduce the binding between crown host and pyridinium guest molecules. This polarization effect, together with the orientation of the substituent and steric factors in the complex, influences the $\pi-\pi$ interaction. In addition, the negative charge on the benzene rings of the crown ether skeleton is enhanced by the ether oxygen atoms. Charge recognition is an electrostatic effect in which the negative face of the aromatic ring interacts with the positive charge of the pyridinium ring. This simple electrostatic view of the interaction predicts that maximizing the positive charge on the pyridinium ring will be favorable for binding.

Table 2 shows that the K_a values are much higher for the crown ether–pyridinium complexes than for the crown ether–substituted pyridinium complexes. Also, the mono-benzene-substituted crown ether complexes have enhanced stability compared with their disubstituted counterparts. However, stability constants are small for all complexes, indicating only weak interaction between host and guest molecules. The differences in stability are a consequence of the steric and electrostatic dissimilarities between the pyridinium ions and the crown ethers. The small pyridinium ring can penetrate deeper into the cavity of the macrocycle than substituted pyridinium ions, and this allows increased interaction between the phenyl ring(s) of the crown ethers and the electron-deficient pyridinium cation. The amino group is smaller than the methyl substituent and can form hydrogen bonds, which explains the greater K_a values for the 1-aminopyridinium complexes than the 1-methylpyridinium complexes. The ^{1}H NMR data indicate that the aromatic–aromatic, $\pi-\pi$, and cation–π interactions play a major role in the complexation between benzene-substituted crown ethers and 1-amino- and 1-methylpyridinium ions, but under favorable conditions hydrogen bonds can enhance the stability of crown ether complexes.

To exclude the influence of $\pi-\pi$ interactions, we investigated the complexation between unsubstituted 18C6 and pyridinium tetrafluoroborate. Recently, Kasmain et al.[17] prepared a solid 18C6–pyridinium chlorochromate (PyClCrO$_3$) 1:1 complex in order to study the oxidation of alcohols. However, no information was given on the thermodynamic parameters or structure of the 18C6–PyClCrO$_3$ complex. The FAB mass spectrum we recorded for 18C6 and pyridinium tetrafluoroborate in NBA matrix showed a peak at $m/z = 344$, which corresponds to that in the 1:1 $[18C6-Py]^+$ complex after loss of its BF_4^- counterion. The ^{1}H NMR chemical shift data indicated formation of a complex in CD_3CN at 298 K. In this 1:1 complex the most significant change in chemical shift was observed for the H2,6 protons of the pyridinium ring. The signal for H2,6 showed a downfield shift, indicative of hydrogen-bonding interactions with host oxygen atoms. The chemical shifts of H4 and H3,5 of the pyridinium ring were almost identical in the free and the complexed form. The unsubstituted crown ether–pyridinium complex is likely stabilized by N^+–H···O hydrogen bonds and possibly also by secondary C–H···O interactions.[26] The measured stability constant of 113 dm^{3}mol^{-1} shows that 18C6–Py is the most stable of the complexes studied. However, in the crystal structures of the 2B18C6–pyridinium complexes (Figures 2 and 4), hydrogen bonding seems to play a secondary role. Obviously, the $\pi-\pi$ interaction is dominant in these complexes, because the benzene rings decrease the negative charge of the oxygen atoms and hence their ability to undergo hydrogen bonding. This is in full agreement with the observed stability constants, which decrease in the order unsubstituted crown ether > benzo-substituted crown ether > dibenzo-substituted crown ether.

To investigate the solvent effect, we studied the complexation of pyridinium tetrafluoroborate with 2B18C6 in $CDCl_3$

by the ^{1}H NMR titration method. A small amount of CD_3CN was added to the $CDCl_3$ solution because pyridinium salts are insoluble in apolar solvents. The stability constant of the crown ether complexes increased with decreasing polarity of the solvent. ^{1}H NMR spectroscopy with the H4 proton of the pyridinium ring as probe revealed a K_a value of 314 (12) dm^3 mol^{-1} [$\Delta\delta_C = 0.59$ (0.03)] in $CDCl_3$ (4 mol % CD_3CN) at 298 K.

True molecular recognition and a physical attraction between host and guest should result in a favorable enthalpy change ($-\Delta H$) on complexation, and in organic media the cation–π effect is primarily enthalpic in origin.[4b] For 2B21C7 and 2B24C8, the enthalpies of complexation were evaluated by means of least-squares fit of $\ln K_a$ versus $1/T$ to give ΔH and the corresponding standard deviations. The accuracy of the resulting thermodynamic values depends on the temperature range, which should be sufficiently narrow to ensure that the variation in the absolute value of the enthalpy is small, but also sufficiently large that the plot can be evaluated with minimum error. A typical compromise is a range of about 30 °C. The enthalpy and entropy values of crown–pyridinium tetrafluoroborate interactions show a small difference between the two ethers. The relevant thermodynamic parameters for the 2B21C7 complex are $\Delta H^\circ = -19$ (2) kJ mol^{-1}, ΔS°(298 K) $= -34$ (6) J mol^{-1} K^{-1}, and for the 2B24C8 complex $\Delta H^\circ = -12.6$ (0.5) kJ mol^{-1}, ΔS°(298 K) $= -18$ (1) J mol^{-1} K^{-1}. It can be concluded from the ΔH° and ΔTS° contributions to the ΔG° value that the complexes are enthalpy stabilized in CD_3CN. This and the overall negative entropy indicate that the cation–π interaction influences the binding of the complexes.

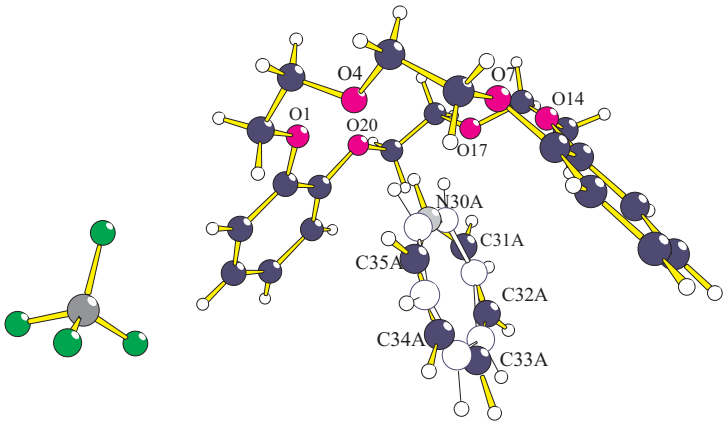

Figure 2. Ball-and-stick representation of the solid-state structure of 2B18C6–pyridinium tetrafluoroborate complex. The disorder of the pyridinium cation is about 0.5. Selected atomic distances [Å] and bond angles [°]: 1) pyridinium ring: N(30A)–C(31A) 1.368(9), N(30A)–C(35A) 1.359(8), C(31A)–C(32A) 1.377(9), C(32A)–C(33A) 1.365(8), C(33A)–C(34A) 1.361(9), C(34A)–C(35A) 1.382(9), C(35A)-N(30A)-C(31A) 120.5(8), N(30A)-C(31A)-C(32A) 121.2(8), C(31A)-C(32A)-C(33A) 118.4(9), C(32A)-C(33A)-C(34A) 120.1(10), C(33A)-C(34A)-C(35A) 121.7(9), C(34A)-C(35A)-N(30A) 118.0(8); 2) crown ether: C(26)–C(8) 6.523, C(21)–C(15) 6.017, C(24)–C(10) 9.592, C(23)–C(11) 9.568, O(1)–O(14) 5.517, O(20)–O(7) 5.580; 3) intermolecular distances: N(30A)–C(13) 3.441, N(30A)–C(8) 3.499, N(30A)–O(14) 3.363, N(30A)–O(7) 3.436, N(30A)–C(26) 3.477, N(30A)–C(21) 3.504, N(30A)–O(1) 3.342, N(30A)–O(20) 3.395, H(30A)–O(1) 2.734, H(30A)–O(4) 2.889, H(30A)–O(7) 3.178, H(30A)–O(14) 3.191, H(30A)–O(17) 3.012, H(30A)–O(20) 2.863, H(35B)–O(4) 2.118, H(30B)–O(17) 2.103.

X-ray crystallography and solid-state complexes: Complexes between 2B18C6 and pyridinium tetrafluoroborate and between 2B18C6 and 1-aminopyridinium tetrafluoroborate were isolated by slow evaporation of solutions. The solid-state structures of the complexes were determined by single-crystal X-ray crystallography. Crystal data and data collection parameters are presented in Table 3.

Crystal structure of the 2B18C6–pyridinium tetrafluoroborate complex: A characteristic feature of the crystal structure of a π–π complex is the presence of stacks of nearly parallel donor and acceptor molecules. Interplanar distances between adjacent donor and acceptor molecules within a stack are somewhat shorter than the van der Waals contact distance (ca. 3.4 Å in aromatic hydrocarbons). The condition of maximum interaction does not usually correspond to the center-on-center donor–acceptor orientation. The angle between the normal to the molecular plane and the stacking axis is 5–30°.[27]

All the features noted above are found in the crystal structure of the 2B18C6–pyridinium tetrafluoroborate complex. As can be see from Figure 2, the atoms of the benzene rings form two planes. The pyridinium ion is located between phenyl substituents at the van der Waals distance, and this interaction is probably the principal factor in the packing of units. Inspection of the crystal packing of the molecules of the complex reveals an array of symmetrically arranged 2B18C6–pyridinium complexes (Figure 3) that form approximately orthogonal alternating units with respect to each other. The array is stabilized by π–π interactions and hydrogen bonds. The interplane separations between the centroids of two phenyl rings are 8.00 Å, and the interplanar separations between π-donor and π-acceptor lie within the range 3.48–5.83 Å. The midpoint distances between the

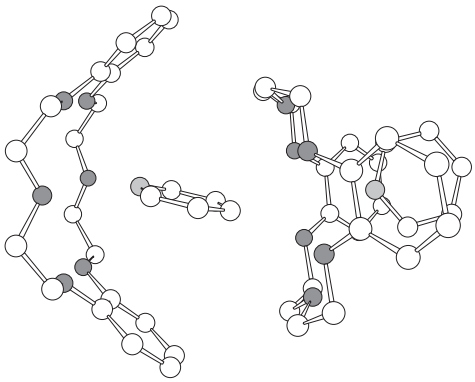

Figure 3. Part of the continuously stacked array of 2B18C6-pyridinium tetrafluoroborate in the crystal. The complex is packed such that the macrocycles form separate channels containing pyridinium cations and tetrafluoroborate anions in the crystallographic *b* direction.

0947-6539/98/0401-0088 $ 17.50+.50/0 *Chem. Eur. J.* **1998**, *4*, No. 1

phenyl and pyridinium rings are 3.94 and 4.60 Å. The single-crystal X-ray structure of the 2B18C6–pyridinium tetrafluoroborate complex shows that the interplanar angles of electron-deficient pyridinium and electron-rich benzene rings are 54 and 26°, and the angle between the two phenyl rings is about 79°. The pyridinium ion is disordered, and, as illustrated in Figure 2, adopts two alternative orientations with almost equal probability [site occupation factors (SOF) of 0.53 and 0.47].

In the crystal structure of the pyridinium complex (Figure 2) the nitrogen atom was assigned to the position close to the macrocycle cavity, since this orientation gave the best results on refinement. The distances between nitrogen atom (N30A) and the oxygen atoms of the macrocycle are 3.39 ± 0.05 Å. On this basis, it is not unreasonable to suggest that N–H···O hydrogen bonding can occur. This bonding would lead to deeper inclusion of the pyridinium unit in the cavity of 2B18C6 and hence enhance overlap between the host and guest π systems. The short distance between O1 and the N–H group (H30A–O1 2.73 Å) supports this conclusion. In solution, however, the ^{1}H NMR results suggest that the N–H group is located outside of the cleft formed by the phenyl rings.

The molecular dimensions of the 2B18C6 ligands are similar to those expected. The mean C–O bond length of the catechol oxygen atoms is 1.37 Å, while the C–O distances for the other oxygen atoms are about 1.43 Å. The aliphatic CH_2–CH_2 bond lengths are 1.47–1.49 Å, but appear to be normal for this type of ligand.[28,29] Most of the dimensions in the benzene ring are normal, but the outermost C–C bond lengths are 1.3654 and 1.3804 Å, again similar to findings in previous analyses of crown complexes.

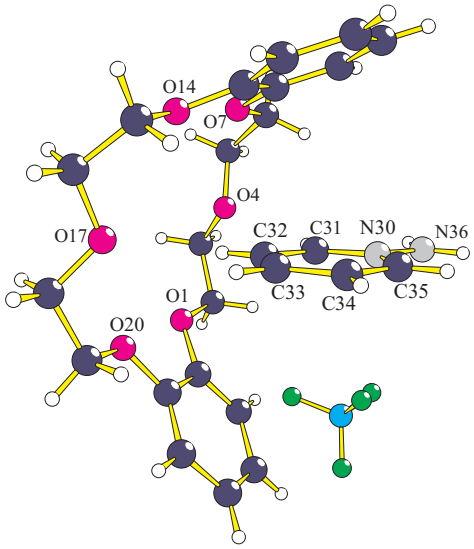

Figure 4. Ball-and-stick representation of the solid-state structure of the complex between 2B18C6 and 1-amino-pyridinium tetrafluoroborate. Selected atomic distances [Å] and bond angles [°]: 1) pyridinium ring: N(36)–N(30) 1.414(5), N(30)–C(31) 1.341(4), C(31)–C(32) 1.357(6), C(32)–C(33) 1.366(6), C(33)–C(34) 1.377(6), C(34)–C(35) 1.359(5), C(35)–N(30) 1.332(5), N(36)–N(30)–C(31) 116.9(3), N(36)-N(30)-C(35) 121.2(3), C(31)-N(30)-C(35) 121.9(3), N(30)-C(35)-C(34) 119.7(3), C(35)-C(34)-C(33) 119.7(4), C(34)-C(33)-C(32) 119.2(4), C(33)-C(32)-C(31) 119.9(3), C(32)-C(31)-N(30) 119.6(3); 2) crown ether: C(26)–C(8) 6.509, C(21)–C(13) 6.520, C(24)–C(9) 8.819, C(23)–C(11) 9.499, O(1)–O(14) 5.541, O(20)–O(4) 4.642; 3) intermolecular distances: C(32)–C(8) 3.430, C(32)–C(13) 3.442, C(32)–C(21) 3.538, C(32)–C(26) 3.549, C(32)–O(1) 3.469, C(32)–O(4) 3.449, C(32)–O(14) 3.398, C(32)–O(17) 3.408, C(35)–C(11) 4.428, C(35)–C(10) 4.318, C(35)–C(23) 5.882, C(35)–C(24) 5.863, H(31)–O(4) 2.471, H(33)–O(17) 2.578, N(30)–C(11) 4.713, N(36)–C(10) 4.697.

Crystal structure of the 2B18C6–1-aminopyridinium tetrafluoroborate complex: The solid-state structure of the 1:1 complex formed between 2B18C6 and 1-aminopyridinium tetrafluoroborate (Figure 4) shows that the electron-deficient 1-aminopyridinium ring system is inserted into the cavity of the macrocycle between two adjacent phenyl substituents. The structure and the superstructure (stacking) are similar those of the 2B18C6–pyridinium complex, suggesting that complexes of benzene-substituted crown ethers with pyridinium ions may in general exhibit a stacking structure provided the size and shape of the acceptor are suitable.

In 2B18C6, the mean planes of the two opposite phenyl substituents are separated by 8.00 Å, and the planes form an angle of 77°. The planes of the pyridinium cation and the phenyl rings form two different angles (22 and 55°). The centroid–centroid distances between the phenyl rings and the pyridinium unit are 3.84 and 4.65 Å, and the shortest intermolecular contact between crown ether and pyridinium ion is 3.43 Å (C8–C38). Despite this somewhat large separation between benzene and pyridinium rings, π–π interaction is a primary force stabilizing the complex. The distances between the oxygen atoms of the polyether chains and the closest carbon atom of the pyridinium ring (C38) vary between 3.40 and 3.47 Å. Inspection of the 2B18C6–1-aminopyridinium ion complex in the crystal reveals a short hydrogen bond interaction between a hydrogen atom of the amino group and O20 (N36–H36A···O20: 2.22 Å, 167°) and two weak, nonlinear C–H···O hydrogen bonds between C–H of the pyridinium ring and ether oxygen atoms (C31–H31···O4: 2.47 Å, 135° and C33–H33···O17: 2.58 Å, 131°). Again the structural features of the macrocyclic ligand are similar to those reported for other polycyclic ether molecules.[28,29] The structure of the complex shows no disorder of the 1-aminopyridinium ring. The amino group points outwards at an angle of about 25° from the vectors through catechol oxygens (Figure 5), allowing hydrogen bonding with the adjacent polyether chain.

Conclusions

Aromatic–aromatic, π–π, and cation–π interactions are among the many noncovalent intermolecular forces that contribute to biological structures. They also play a significant role in self-assembly processes when large ordered nanometer-scale structures are formed selectively from relatively small molecular compounds. Pyridinium ring systems occur in many natural products, including nicotine, nicotinic acid, and pyridoxine (vitamin B_6). In addition, nicotinamide adenine dinucleotide (NAD^+) is an important and widespread redox coenzyme that owes its reactivity to the pyridinium moiety.

  0947-6539/98/0401-0089 $ 17.50+.25/0

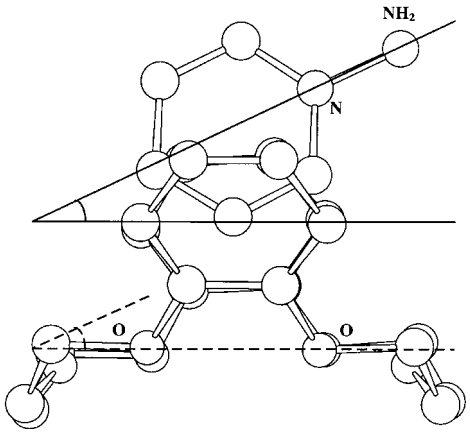

Figure 5. X-ray crystal structure of 2B18C6–1-amino-pyridinium complex showing the position and direction of the amino group.

Our studies emphasize the stabilizing interactions between positively charged organic guests and the electron-rich face of an aromatic ring in crown ethers. The research described here has shown that benzene-substituted crown ethers form stable 1:1 complexes with electron-deficient pyridinium cations. Benzene-substituted crown ether–pyridinium cation complexes can be detected and studied in gas, solution, and solid state. The present results indicate that the complexes are stabilized by $\pi-\pi$ and cation–π interactions. The X-ray crystal structure analyses reveal the characteristic features of $\pi-\pi$ interactions: the structures contain partially offset nearly parallel (twist angle 25°) cofacial arrangements of pyridinium phenyl rings, with approximate interplane separations of 3.4–4.6 Å. We have demonstrated that simple macrocyclic polyethers with phenyl substituents can provide attractive host compounds for the study of weak noncovalent interactions with aromatic organic cations such as tropylium[11,30] and pyridinium ions.

Experimental Section

Materials and methods: Acetonitrile (Fluka), CD_3CN (CEOL C.E.), dichloromethane (Lab-Scan), 1,2-dichloroethane (Lab-Scan), diethyl ether (Fluka), diethyl acetate (Lab-Scan) and pyridine (Fluka) were dried and distilled according to literature procedures.[31] Dibenzo-24-crown-8 (2B24C8, Fluka) was purified by dissolving in MeOH and precipitation by addition of water (m.p. 104 °C). The following crown ethers were obtained from the indicated suppliers and used without further purification: benzo-15-crown-5 (1B15C5), benzo-18-crown-6 (1B18C6), dibenzo-21-crown-7 (2B21C7), and 18-crown-6 (all Fluka), dibenzo-18-crown-6 (2B18C6, Parish Chemical Co), and dibenzo-30-crown-10 (2B30C10, Aldrich). All other reagents, unless otherwise noted, were obtained from Fluka and were used without further purification.

^{1}H and ^{13}C NMR spectra were recorded on a Bruker AM 200 spectrometer. NMR chemical shifts are reported relative to internal TMS. EI and FAB mass spectra were obtained on a Kratos MS 80 mass spectrometer with the DART data system. The UV–Vis spectra were recorded with a Phillips PU 8740 spectrophotometer. Small amounts of the compounds were accurately weighed with a Perkin–Elmer AD-2 autobalance. Elemental analysis was carried out with a Perkin–Elmer 2400. Melting points were determined with a Thermopan microscope (Reichert, Vienna) and are uncorrected.

Pyridinium tetrafluoroborate was prepared according to literature procedures from pyridine and tetrafluoroboric acid (HBF_4), which was dried with Sikkon ($CaSO_4$, Fluka).[32] M.p. 203 °C; ^{1}H NMR (200 MHz, CD_3CN, 25 °C, TMS): $\delta = 8.73$ (m, $^3J(H,H) = 5.25$ Hz, 2H, H2,6), 8.63 (m, $^3J(H,H) = 7.87$ Hz, 2H, H4), 7.07 (m, 1H, H3,5), 7.11 (s, 1H, NH); FABMS (NBA): m/z (%) = 80 (100) $[M-BF_4]^+$. The ^{1}H NMR spectrum was in accordance with that reported in the literature.[33]

1-Aminopyridinium tetrafluoroborate was prepared from pyridine and hydroxylamine-*o*-sulfonic acid[34] by the method of Gösl and Meuwsen[35] slightly modified. The desired tetrafluoroborate salt was prepared by action of tetrafluoroboric acid instead of hydriodic acid. M.p. 143 °C; ^{1}H NMR (200 MHz, CD_3CN, 25 °C, TMS): $\delta = 8.56$ (m, $^3J(H,H) = 5.38$ Hz, 2H, H2,6), 8.29 (m, $^3J(H,H) = 7.87$ Hz, 2H, H4), 7.93 (m, $^4J(H,H) = 1.76$ Hz, 1H, H3,5), 7.04 (s, 2H, NH_2); FABMS (NBA): m/z (%) = 95 (100) $[M-BF_4]^+$.

1-Methylpyridinium iodide was prepared as described elsewhere.[36] M.p. 118 °C; ^{1}H NMR (200 MHz, CD_3CN, 25 °C, TMS): $\delta = 8.76$ (m, $^3J(H,H) = 5.87$ Hz, 2H, H2,6), 8.51 (m, $^3J(H,H) = 7.85$ Hz, 2H, H4), 8.03 (m, 1H, H3,5), 4.35 (s, 3H, CH_3).

1-Methylpyridinium tetrafluoroborate was prepared by treating 1-methylpyridinium iodide with excess of boron trifluoride etherate under a dry nitrogen atmosphere.[37] M.p. 14 °C; ^{1}H NMR (200 MHz, CD_3CN, 25 °C, TMS): $\delta = 8.64$ (m, $^3J(H,H) = 5.74$ Hz, 2H, H2,6), 8.49 (m, $^3J(H,H) = 7.86$ Hz, 2H, H4), 8.01 (m, 1H, H3,5), 4.31 (s, 3H, CH_3); FABMS (NBA): m/z (%) = 94 (100) $[M-BF_4]^+$.

General procedure for the synthesis of solid crown ether–pyridinium tetrafluoroborate complex: Crown ether (0.25 mmol) and pyridinium salt (0.25 mmol) were dissolved in MeCN (4 cm^3). EtO_2 was used to precipitate the solid complex, which was collected by filtration.

Fast atom bombardment mass spectrometry (FABMS): Argon was used to provide the primary beam of atoms, and samples were mixed with a small amount of 3-nitrobenzyl alcohol (NBA, Aldrich) matrix on a stainless steel probe. Spectra were recorded in the positive-ion mode.

General method of computing stability constants by ^{1}H NMR titration: The solubilities of the molecules studied placed some limits on the choice of NMR solvents. Deuterated acetonitrile was chosen as primary solvent because it is polar with a moderately high polarity parameter ($E_T^N = 0.460$[38]) and dissolves all species of interest. A standard solution of pyridinium salt in CD_3CN was prepared with the concentration of acceptor just sufficient to give an observable NMR signal [$(4-10)\times10^{-4}$ M]. A small amount of TMS (Aldrich) was added as internal standard. A series of donor solutions (6–10) was made by weighing out an appropriate amount of donor (0.1–0.01 M). A 2–4 mL portion of the standard solution was then added, and the flask was reweighed. After initial preparation of the samples a portion was transferred to a sample tube (5 mm). The tube was sealed with parafilm and capped with a plastic top, and the spectra were recorded immediately to avoid evaporation. The temperature was held constant within ± 0.3 K. The stability constant K_a for 1:1 complexation was calculated from the NMR chemical shifts [Eq. (1)], where C_A and C_D are

$$C_D/\Delta\delta_{obs} = [1/\delta_C - \delta_A)](C_A + C_D - C_C) + 1/K_a(\delta_C - \delta_A) \quad (1)$$

$$1/\delta_{obs} = 1/K_a(\delta_C - \delta_A)C_D + 1/(\delta_C - \delta_A) \quad (2)$$

concentrations of acceptor and donor, $\Delta\delta_{obs} = \delta_{obs} - \delta_A$, δ_{obs} is the observed NMR shift of a specific acceptor proton (or an equivalent set) in the equilibrium solution, and δ_A is the shift of the free acceptor proton. Equation (1) contains two unknown terms, concentration of the complex C_C and the shift of the complex proton δ_C, which can be calculated by means of a simple iterative procedure based on successive approximations. If $C_D \gg C_A$, Equation (1) reduces to the equivalent relationships given by Equation (2), the Benesi–Hildebrand form.[39]

The errors in K_a and $\Delta\delta_C$ were evaluated numerically by standard deviations of single K_a and $\Delta\delta_C$ values usually obtained from six to eight measurements. The regression values for the least-squares fitting [Eq. (2)] were generally better than 0.99.

X-ray crystal structure analysis. X-ray diffraction measurements were performed on an Enraf–Nonius CAD4 diffractometer with graphite-monochromatized $Mo_{K\alpha}$ radiation and $\omega/2\theta$ scan mode. Table 3 summa-

0947-6539/98/0401-0090 $ 17.50+.50/0 *Chem. Eur. J.* **1998**, *4*, No. 1

Table 3. Crystal data and data collection parameters.

	2B18C6 – $PyBF_4$	2B18C6 – 1-NH_2-$PyBF_4$
formula	$C_{25}H_{30}B_1F_4N_1O_6$	$C_{25}H_{31}B_1F_4N_2O_6$
M_r	527.31	542.33
T (K)	296 ± 2	296 ± 2
wavelength (Å)	$\lambda(Mo_{K\alpha}) = 0.71069$	$\lambda(Mo_{K\alpha}) = 0.71069$
crystal system	monoclinic	monoclinic
space group	*Cc*	*Cc*
a (Å)	18.327(3)	18.303(4)
b (Å)	13.3380(12)	13.179(3)
c (Å)	14.099(2)	13.841(2)
α (°)	90.000	90.000
β (°)	133.353(10)	129.20(2)
γ (°)	90.000	90.000
volume (Å^3)	2506.0(5)	2587.3(9)
Z	4	4
ρ_{calcd} (g cm^{-3})	1.398	1.392
μ ($Mo_{K\alpha}$, mm^{-1})	0.272	0.117
F(000)	1104	1136
crystal size (mm)	$0.25 \times 0.45 \times 0.45$	$0.25 \times 0.35 \times 0.45$
θ range (°)	2.11 – 24.97	2.11 – 24.97
index ranges	$0 \le h \le 21$, $0 \le k \le 15$, $-16 \le l \le 16$	$0 \le h \le 21$, $0 \le k \le 15$, $-16 \le l \le 16$
reflections collected	2282	2352
independent reflections	2282	2352
refinement method	Full-matrix least-squares on F^2	
data/restraints/parameters	2282/170/390	2352/2/344
GoF S	1.034	1.043
final R indices [$I > 2\sigma(I)$]	$R_1 = 0.0406$, $wR_2 = 0.1192$	$R_1 = 0.0389$, $wR_2 = 0.1108$
R indices (all data)	$R_1 = 0.0561$, $wR_2 = 0.1321$	$R_1 = 0.0527$, $wR_2 = 0.1204$
extinction coefficient	0.0073(12)	0.0100(12)
largest diff. peak/hole (e Å^{-3})	0.322/ – 0.230	0.355/ – 0.200

rizes the crystal data, data collection, and refinement parameters for complexes 2B18C6 – pyridinium tetrafluoroborate and 2B18C6 – 1-aminopyridinium tetrafluoroborate. The structures were solved by direct methods with the SHELXS program system[40] and subjected to full-matrix refinement with SHELXL-93.[41]

2B18C6-pyridinium tetrafluoroborate complex: Single crystals suitable for X-ray crystallography were grown by slow evaporation of an equimolar solution of 2B18C6 and pyridinium tetrafluoroborate in a 5:3 mixture of CH_2Cl_2 and MeCN. $C_{25}H_{30}BF_4NO_6$ (527.31): calcd C 56.94, H 5.73, N 2.66; found C 56.70, H 5.70, N 2.66.

2B18C6-1-aminopyridinium tetrafluoroborate complex: Single crystals suitable for X-ray crystallography were grown by slow evaporation of an equimolar solution of 2B18C6 and 1-aminopyridinium tetrafluoroborate in a 5:1 mixture of CH_2Cl_2 and MeCN. $C_{25}H_{31}BF_4N_2O_6$ (542.33): calcd C 55.37, H 5.76, N 5.17; found C 55.05, H 5.71, N 5.20.

Crystallographic data (excluding structure factors) for the structure reported in this paper have been deposited with the Cambridge Crystallographic Data Centre as supplementary publication no. CCDC-100664. Copies of the data can be obtained free of charge on application to CCDC, 12 Union Road, Cambridge CB21EZ, UK (Fax: Int. code + (1223) 336-033; e-mail: deposit@ccdc.cam.ac.uk).

Acknowledgements: We thank Päivi Joensuu for the mass spectra, and the Trace Element Laboratory, University of Oulu, for the elemental analyses.

Received: June 20, 1997 [F734]

[1] F. Diederich, *Cyclophanes*, The Royal Society of Chemistry, Cambridge, **1991**, p. 246.

[2] a) W. Saenger, *Principles of Nucleic Acid Structure*, Springer, New York, **1984**, pp. 132 – 140; b) S. K. Burley, G. A. Petsko, *Science* **1985**, *229*, 23 – 29; see also T. Blundell, J. Singh, J. Thornton, S. K. Burley, G. A. Petsko, *ibid.* **1986**, *234*, 1005; c) L. Serrano, M. Bycroft, A. R. Fersht, *J. Mol. Biol.* **1991**, *218*, 465 – 475; d) C. A. Hunter, J. Singh, J. M. Thornton, *ibid.* **1991**, *218*, 837 – 846.

[3] a) C. A. Hunter, J. K. M. Sanders, *J. Am. Chem. Soc.* **1990**, *112*, 5525 – 5354; b) C. Chipot, R. Jaffe, B. Maigret, D. A. Pearlman, P. A. Kollman, *J. Am. Chem. Soc.* **1996**, *118*, 11217 – 11224.

[4] a) S. C. Zimmerman, M. Mrksich, M. Balogna, *J. Am. Chem. Soc.* **1989**, *111*, 8528 – 8530; b) D. A. Stauffer, R. E. Barrans, D. A. Dougherty, *J. Org. Chem.* **1990**, *55*, 2762 – 2767; c) S. P. Ferguson, E. M. Sanford, E. M. Seward, F. Diederich, *J. Am. Chem. Soc.* **1991**, *113*, 5410 – 5419; d) A. McCurdy, L. Jimenez, D. A. Stauffer, D. A. Dougherty, *J. Am. Chem. Soc.* **1992**, *114*, 10314 – 10321; e) S.-H. Lee, K. Imamura, J. Otsuki, K. Araki, M. Seno, *J. Chem. Soc. Perkin Trans 2* **1996**, 847 – 852.

[5] P. R. Ashton, E. J. T. Chrystal, J. P. Mathias, K. P. Parry, A. M. Z. Slawin, N. Spencer, J. F. Stoddart, D. J. Williams, *Tetrahedron Lett.* **1987**, *50*, 6367 – 6370.

[6] a) F. M. Raymo, J. F. Stoddart, *Chem. Ber.* **1996**, *129*, 981 – 990; b) P. T. Glink, C. Schiavo, J. F. Stoddart, D. J. Williams, *Chem. Commun.* **1996**, 1483 – 1490; c) P. R. Ashton, R. Ballardini, V. Balzani, S. E. Boyd, A. Credi, M. T. Gandolfi, M. Gómez-López, S. Iqbal, D. Philp, J. A. Preece, L. Prodi, H. G. Ricketts, J. F. Stoddart, M. S. Tolley, M. Venturi, A. J. P. White, D. J. Williams, *Chem. Eur. J.* **1997**, *3*, 152 – 170 and references therein.

[7] R. Móeric, J. P. Vigneron, J.-M. Lehn, *J. Chem. Soc. Chem. Commun.* **1993**, 129 – 131.

[8] a) D. A. Dougherty, D. A. Stauffer, *Science* **1990**, 250, 1558 – 1560; b) P. C. Kearney, L. S. Mizoue, R. A. Kumpf, J. E. Forman, A. McCurdy, D. A. Dougherty, *J. Am. Chem. Soc.* **1993**, *115*, 9907 – 9919. c) A recent review on cation – π interactions: J. M. Ma, D. A. Dougherty, *Chem. Rev.* **1997**, *97*, 1303 – 1324.

[9] a) J. L. Sussman, M. Harel, F. Frolow, C. Oefner, A. Goldman, L. Toker, I. Silman, *Science* **1991**, *253*, 872 – 879; b) D. A. Dougherty, *Science* **1996**, *271*, 163 – 168.

[10] a) K. Araki, H. Shimizu, S. Shinkai, *Chem. Lett.* **1993**, 205 – 208; b) J. W. Caldwell, P. A. Kollman, *J. Am. Chem. Soc.* **1995**, *117*, 4177 – 4178.

[11] a) M. Lämsä, J. Pursiainen, K. Rissanen, J. Huuskonen, *Acta Chem. Scand.* **1997**, in press; b) M. Lämsä, T. Suorsa, J. Pursiainen, J. Huuskonen, K. Rissanen, *Chem. Commun.* **1996**, 1443 – 1444.

[12] L. Stryer, *Biochemistry*, 3rd ed., W. H. Freeman, New York, **1988**, p. 320.
[13] a) K. M. Harmon, *Carbonium Ions*, *Vol. IV* (Eds. G. A. Olah, P. von R. Schleyer), Wiley, New York, **1973**, p. 1579; b) J. W. Bunting, M. M. Conn, *Can. J. Chem*. **1990**, *68*, 537 – 542.
[14] O. Pieppers, R. M. Kellogg, *J. Chem. Soc. Chem. Commun.* **1980**, 1154 – 1155.
[15] a) P. C. Kearney, L. S. Mizoue, R. A. Kumpf, J. E. Forman, A. McCurdy, D. A. Dougherty, *J. Am. Chem. Soc*. **1993**, *115*, 9907 – 9919; b) R. Móeric, J.-P. Vigneron, J.-M. Lehn, *J. Chem. Soc. Chem. Commun.* **1993**, 129 – 131.
[16] a) G. D. Iasi, B. Masci, *Tetrahedron Lett*. **1993**, *34*, 6635 – 6639; b) F. Inokuchi, K. Araki, S. Shinkai, *Chem. Lett*. **1994**, 1383 – 1386.
[17] H. S. Kasmai, S. G. Mischke, T. J. Blake, *J. Org. Chem.* **1995**, *60*, 2267 – 2270.
[18] K. K. Laali, *J. Phys. Org. Chem*. **1994**, *7*, 465 – 478.
[19] M. Vincenti, C. Minero, E. Pelizzetti, A. Secchi, E. Dalcanale, *Pure Appl. Chem.* **1995**, *67*, 1075 – 1084.
[20] M. Sawada, Y. Okumura, M. Shizuma, Y. Takai, Y. Hidaka, H. Yamada, T. Tanaka, T. Kaneda, K. Hirose, S. Misumi, S. Takahashi, *J. Am. Chem. Soc*. **1993**, *115*, 7381 – 7388, and references therein.
[21] M. Lämsä, T. Kuokkanen, J. Jalonen, P. O. I. Virtanen, *J. Phys. Org. Chem*. **1995**, *8*, 377 – 384.
[22] For a critical evaluation of FABMS analysis, see G. J. Langley, D. G. Hamilton, M. C. Grossel, *J. Chem. Soc. Perkin Trans. 2* **1995**, 929 – 933.
[23] T. Wang, J. S. Bradshaw, R. M. Izatt, *J. Heterocycl. Chem*. **1994**, *31*, 1097 – 1114.
[24] K. A. Connors, *Binding Constants*, John Wiley, New York, **1987**, pp. 189 – 200.
[25] Wavefunction, Irvine, CA (USA), 1996.
[26] For examples and a detailed discussion of the hydrogen bond properties of C – H ··· O interactions, see T. Steiner, *Chem. Commun.* **1997**, 727 – 734.
[27] M. Pasternak, T. Sonnino, *Molecular Interactions*, *Vol. 2*. (Eds. H. Ratajczah, W. J. Orville-Thomas), Wiley, Chichester, **1981**, p. 455.
[28] D. L. Hughes, *J. Chem. Soc. Dalton Trans.* **1975**, 2374.
[29] I. R. Hanson, D. L. Hughes, D. L. Truter, *J. Chem. Soc. Perkin Trans. 2*, **1976**, 972 – 976.
[30] M. Lämsä, T. Kuokkanen, *J. Phys. Org. Chem*. **1996**, *9*, 21 – 28.
[31] D. D. Perrin, W. L. F. Armarego, D. R. Perrin, *Purification of Laboratory Chemicals*, 3rd ed., Pergamon, Oxford, **1988**.
[33] R. Daniels, C. G. Kormendy, *J. Org. Chem*. **1962**, *27*, 1860.
[33] P. Sandor, L. Radics, *Org. Magn. Reson*. **1980**, *14*, 98 – 102.
[34] H. J. Matsuguma, L. F. Audrieth, *Inorg. Synth.* **1957**, *5*, 122 – 125.
[35] R. Gösl, A. Meuwsen, *Org. Synth*. **1973**, *5*, 43 – 45.
[36] F. G. Mann, F. C. Baker, *J. Chem. Soc.* **1961**, 3845 – 3851.
[37] P. F. Donovan, D. A. Conley, *J. Chem. Eng. Data* **1966**, *11*, 614 – 615.
[38] C. Reichardt, *Solvents and Solvent Effects in Organic Chemistry*, VCH, Weinheim, **1988**, p. 408.
[39] H. A. Benesi, J. H. Hildebrand, *J. Am. Chem. Soc.* **1949**, *71*, 2703 – 2704.
[40] G. M. Sheldrick in *Crystallographic Computing 3*, (Eds.: G. M. Sheldrick, C. Krüger R. Goddard), Oxford University Press, Oxford, (UK), **1985**, pp. 175 – 189.
[41] G. M. Sheldrick, *SHELXL-93*, Program for the Refinement of Crystal Structure, University of Göttingen, **1993**.

0947-6539/98/0401-0092 $ 17.50+.50/0 *Chem. Eur. J.* **1998**, *4*, No. 1